Maximum Allowable Current Determination of Arbitrary Reconfigurable Battery Systems By Using a Directed Graph Model Combined with Greedy Algorithm

3057761608

June 26, 2023

Abstract

Reconfigurable Battery Systems (RBSs) offer a promising alternative to traditional battery systems owing to their flexible and dynamic changeable topologic structure subjected to battery cell charging and discharging strategies. During the operation of the RBS, Maximum Allowable Current (MAC) is a critical indicator to guide the reconfiguring control of the system in terms of safety and reliability. In this paper, the MAC of the RBS is calculated by using a greedy algorithm based on the directed graph model of the RBS. The effectiveness of this method is validated on a more complex RBS structure based on two proposed structure. This proposed Greedy-based method paves the way for more flexible design and more complex application scenarios, such as battery cell isolation, for RBS.

keywords: Reconfigurable Battery System, Maximum Allowable Current, Greedy Algorithm

1 Introduction

Battery Energy Storage Systems (BESSs) are widely used to store and release high-quality electrical energy in various applications, such as smart grids and wind power plants [1, 2, 3, 4]. Typically, a BESS consists of numerous battery cells that are interconnected by series-parallel circuitry to provide the required capacity storage. The traditional BESS, in which the batteries are connected in a fixed topology, has a significant weakness on its worst battery, caused by the so-called cask effect. Furthermore, if this worst battery is failed during the operation process, it will exacerbate the degradation of the other batteries with a high possibility, and arouse reliability and even safety issues [5, 6].

Reconfigurable Battery System (RBS), which can dynamically switch to different circuit topology configurations as required, is expected to solve the above problem[7]. The ability of switching circuit helps to isolate unhealthy batteries, and thereby improve the safety and reliability of the battery system. Fig. 1

shows two popular typologies of the RBSs developed by Lawson[8] and Visairo [9] respectively. Taking the RBS shown in Fig. 1b as example, the batteries in the RBS can be connected not only in series when the switches S_1, S_5, S_6, S_7, S_8, S_9, and S_{13} are closed, but also in parallel when S_1, S_2, S_3, S_4, S_5, S_9, S_{10}, S_{11}, S_{12}, and S_{13} are closed. Furthermore, when an unhealthy battery, for instance the orange one in Fig. 1a, exits in the RBS, it can be isolated by closing its three adjacent switches (i.e. S_5, S_7 and S_8) and opening the switch below that battery (i.e. S_6) to ensure the system still remains a reliable working mode.
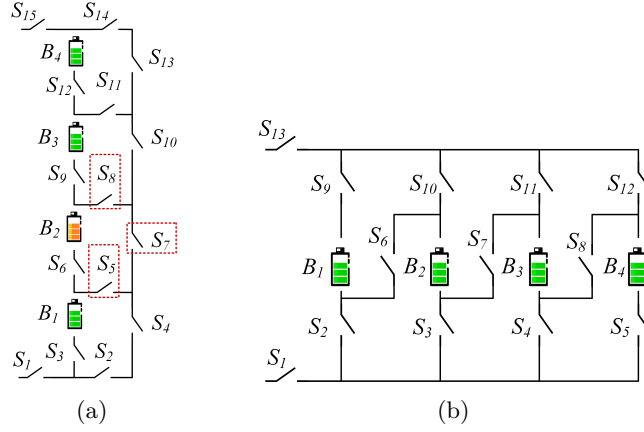

Figure 1: The RBS structure proposed by (a)Lawson[8], (b)Visairo[9].

The complex connecting structure between batteries and switches enables the flexibility of the RBS, but on the other hand brings the challenges in desgin and control cost as well. All switches of the RBS need to be controlled to output currents and powers that match the external load in read-time while avoiding batteries short-circuit. The Maximum Allowable Current (MAC) of the RBS system is defined as the maximum current that is allowed for each individual battery of the system, and is a critical indictor to be evaluate the RBS output current to the electronic appliances.It helps the designer to assess whether the RBS meets the output current requirements, and contributes to the formulation of appropriate and safe management stragegies for the battery management system (BMS). Despite its importance, there is currently no way to automatically evaluate MAC for RBSs. Especially when one (or more) stochastic battery is isolated, it is not possible to simultaneously determine the MAC of the rest of the RBS to assist the BMS to provide a timely adjustment of the control strategy. Under such circumstance, a universal and effective method for calculating the MAC of the RBS is urgently needed for the practical application of RBSs. To achieve this, a directed graph model that builds the relationship between RBS circuit topology and internal resistance and voltage of its batteries are established. Then, a greedy algorithm is employed to search the available circuit

of the RBS for reaching the MAC. With this proposed method, the MAC of RBSs with arbitrary structures can be calculated effectively, including application scenarios with isolated battery cells.

The remainder of this paper is organized as follows: Section II presents the framework and details of the proposed topologic model and the greedy algorithm. In Section III, a case study of using the proposed model and algorithm to enumerate the MAC of a new and complex structure is demonstrated. The calculation results and scenarios such as battery cells isolation also are discussed. Finally, the concluding remarks are drawn in Section IV.

2 Methodology

The central principle of this method is to make the batteries in RBS connected in series as much as possible, thereby maximizing the output current of the RBS. To universally and automatically achieve this, the overall process is divided into four steps, as shown in Fig. 2a. Firstly, a directed graph model is established for subsequent computing, which not only contains the connected relationships between batteries and switches, but also retains the performance parameters of the batteries. Subsequently, based on the equivalent circuit, the MAC problem is transformed into specific objective functions and constraints. Then, the shortest paths (SPs, where additional batteries and switches on the path are penalized as distance) for the batteries are obtained using the Dijkstra algorithm to guide the batteries in the RBS connect in series. Finally, a greedy algorithm is employed to organize the switches, allowing the batteries to connect via their SPs while satisfying the constraints, resulting in the MAC of the RBS.

2.1 Directed graph Model

He et al. [?] once proposed an abstracted directed graph model for RBS, where the nodes represented the batteries, the edges represented the configuration flexibility, and the weight of each vertex corresponded to the battery voltage (Fig. 3a). The model effectively captured all potential system configurations and offered a direct metric for configuration flexibility, but it did not specify the physical implementation of the connectivity between batteries, meaning one graph might have had multiple RBS structures. We previously proposed a novel directed graph model that, in contrast to He's model, used nodes to represent the connections between batteries and switches, and directed edges to represent batteries and switches (Fig. 3b), allowing for a one-to-one correspondence between the RBS structure and the directed graph model. This model was able to accurately and comprehensively represent the RBS topological structure but could not be used for quantitative MAC calculations due to the lack of consideration for battery and switch performance parameters. To address this, an improved directed graph model is used here based on our original model, adding electromotive force and resistance attributes on the edges based to equivalent circuits (Fig. 3c). The model also considers the external load as an equivalent
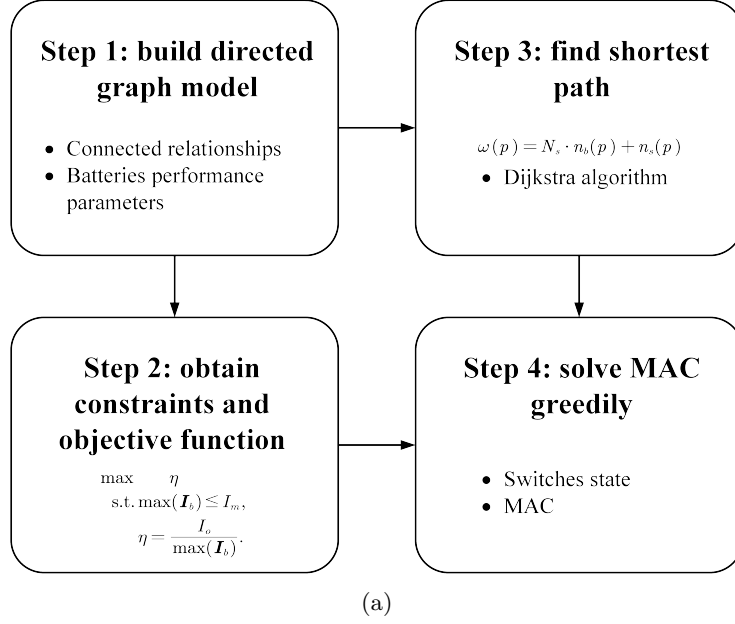
3

Step 1: build directed graph model

- Connected relationships
- Batteries performance parameters

Step 3: find shortest path

$$\omega(p) = N_s \cdot n_b(p) + n_s(p)$$

- Dijkstra algorithm

Step 2: obtain constraints and objective function

$$\max \quad \eta$$
$$\text{s.t.} \max(\boldsymbol{I}_b) \leq I_m,$$
$$\eta = \frac{I_o}{\max(\boldsymbol{I}_b)}.$$

Step 4: solve MAC greedily

- Switches state
- MAC

(a)

Figure 2: Diagram of this method, which contains four main steps.
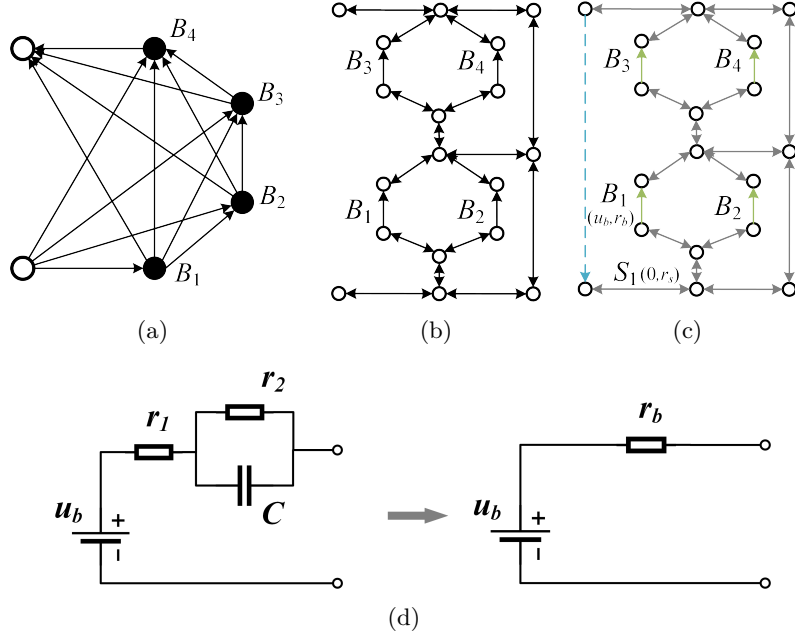

(a)　　　　　　(b)　　　　　　(c)

(d)

Figure 3: Directed graph models used in (a) He's work [**?**], (b) our previous work , and (c) this paper. (d) The equivalent circuit of a battery in this method.

resistance and integrate it into the analysis, making it a complete circuit model for later circuit analysis. The following will provide a detailed explanation of the method for equating the components in RBS and constructing the directed graph model.

In order to use circuit analysis methods to solve the MAC of the RBS, the components in the RBS are equated to ideal circuit elements. As shown in Fig. 3d, the battery in the RBS can be represented as a black-box circuit consisting of two resistors (i.e., r_1 and r_2) and a capacitor (i.e., C), known as the Thevenin model[10, 11]. With an emphasis on the stable output of the RBS, the capacitor in the Thevenin model can be considered as an open circuit without affecting the steady-state current. Therefore, the battery i in the RBS can be simplified as the series connection between a constant voltage source u_i and a resistor r_i. Furthermore, the state of switch j in the RBS is represented by a binary variable x_j, where 0 is for ON and 1 is for OFF, respectively. When the switch is closed, it can be regarded as a resistor with a very small resistance value r_j. Lastly, the external load is considered as a resistor with a value of R_o.

For a given RBS structure, the directed graph model for the RBS is constructed as a directed graph $G(V, E)$ in such a way that:

1. Nodes: The nodes in the directed graph correspond to the connection points of components in the actual RBS. Assuming there are a total of N nodes in the RBS, for the sake of convenience, the anode of the RBS is denoted as v_1 and the cathode as v_N.

2. Edges: The edges in the directed graph correspond to the batteries, switches, and external electrical loads in the actual RBS. Therefore, there are three types of directed edges. For a battery B_i, its directed edge e_i is drawn from the cathode to the anode, as the battery only allows current to flow in one direction when in operation. For a switch S_j, since it is allowed to work under bi-directional currents, it is represented by a pair of directed edges with two-way directions. Regarding the external electronic load, as it is connected to the anode and cathode of the RBS, a directed edge from v_N to v_1 is used to represent it. In conclusion, for a given RBS structure with N_b batteries and N_s switches, the total number of directed edges is $N_b + 2N_s + 1$, where 1 refers to the external electrical load.

3. Edges' attributes: Each edge is assigned two attributes, voltage difference and resistance, based on the equivalent method mentioned above. The values for the battery B_i, switch S_j, and external loads correspond to (u_i, r_i), $(0, r_j)$, and $(0, R_o)$, respectively.

2.2 Constraints and Objective Function

Based on the definition of MAC, determining the MAC of RBS involves maximizing the RBS output current while ensuring that the currents of all batteries do not exceed the batteries' maximum allowable current. In this subsection, the constraints and objective function to solve the RBS's MAC will be established

through circuit analysis, based on the previously constructed directed graph model.

First, the topology in the directed graph model is represented in matrix form $\boldsymbol{A}$, known as the incidence matrix , to facilitate circuit analysis. The specific definition of the incidence matrix is shown in Eq. 1.

$$a_{kl} = \begin{cases} 1, & \text{edge } l \text{ leaves node } k, \\ -1, & \text{edge } l \text{ enters node } k, \\ 0, & \text{otherwise.} \end{cases} \tag{1}$$

For a directed graph consisting of N nodes and $N_b + 2N_s + 1$ directed edges, its incidence matrix $\boldsymbol{A}$ is an $N \times (N_b + 2N_s + 1)$ matrix. In this matrix, the rows and columns represent the nodes and edges of the directed graph, respectively. By distinguishing the components in the RBS corresponding to each column , $\boldsymbol{A}$ can be rewritten as:

$$\boldsymbol{A} = \begin{bmatrix} \boldsymbol{A}_b & \boldsymbol{A}_s & \boldsymbol{A}_o \end{bmatrix}, \tag{2}$$

where $\boldsymbol{A}_b$, $\boldsymbol{A}_s$ and $\boldsymbol{A}_o$ are the sub-matrices corresponding to the batteries, switches and external electrical load, respectively. To alleviate computational complexity, matrix $\boldsymbol{A}$ undergoes dimensionality reduction. Since each directed edge has one node to leave and one to enter, the sum of the values in every column of $\boldsymbol{A}$ is zero. Therefore removing any single one row will not result in a loss of information. Without loss of generality, the last row is removed here. On the other hand, since each switch in the RBS is represented by a pair of directed edges with two-way directions, the two columns corresponding to the switch are mutually opposite. Thus, for the sub-matrix $\boldsymbol{A}_s$, only one column is retained for each pair of columns representing the same switch. As a result, $\boldsymbol{A}$ can be reduced to a $(N-1) \times (N_b + N_s + 1)$ matrix, denoted as $\tilde{\boldsymbol{A}}$, for further calculation of current and voltage. Similar to Eq. 2, $\tilde{\boldsymbol{A}}$ can be rewritten as:

$$\tilde{\boldsymbol{A}} = \begin{bmatrix} \tilde{\boldsymbol{A}}_b & \tilde{\boldsymbol{A}}_s & \tilde{\boldsymbol{A}}_o \end{bmatrix}. \tag{3}$$

After obtaining the incidence matrix, the currents of all batteries and output in RBS are determined by solving the circuit equations. According to Kirchhoffs law, we have

$$\begin{cases} \tilde{\boldsymbol{A}}\boldsymbol{I} = \boldsymbol{0}, \\ \boldsymbol{U} = \tilde{\boldsymbol{A}}^{\mathrm{T}}\boldsymbol{U}_n, \end{cases} \tag{4}$$

where $\boldsymbol{I}$ and $\boldsymbol{U}$ indicate the current and voltage difference arrays of the $N_b + N_s + 1$ edges, respectively; $\boldsymbol{U}_n$ is the voltage array of the $N - 1$ nodes. These directed edges are treated as generalized branches and expressed in matrix form as follows

$$\boldsymbol{I} = \boldsymbol{Y}\boldsymbol{X}\boldsymbol{U} - \boldsymbol{Y}\boldsymbol{X}\boldsymbol{U}_s + \boldsymbol{I}_s, \tag{5}$$

where $\boldsymbol{U}_s$ and $\boldsymbol{I}_s$ denote the source voltage and source current of the generalized branches, respectively. Because all batteries have been equivalent to voltage

sources rather than current sources in the previous subsection, all elements of the array $\boldsymbol{I}_s$ are 0, while the elements of the array $\boldsymbol{U}_s$ are equal to the first attribute of the corresponding edges in the directed graph. The $\boldsymbol{Y}$ in 5 is the admittance matrix of the circuit, defined as the inverse of the impedance matrix. That is the elements of the diagonal matrix $\boldsymbol{Y}$ are equal to the reciprocal of the second attribute of the corresponding edges in the directed graph, and the off-diagonal elements are 0. The $\boldsymbol{X}$ is the state matrix, which describes whether the RBS batteries and switches are allowed to pass current. It is defined as

$$\boldsymbol{X} = \mathrm{diag}(\underbrace{1, 0 \cdots, 1}_{N_b \text{ of } 0/1}, \underbrace{1, 0 \cdots, 1}_{N_s \text{ of } 0/1}, 1) = \begin{bmatrix} \boldsymbol{X}_b & & \\ & \boldsymbol{X}_s & \\ & & 1 \end{bmatrix}. \tag{6}$$

Where the elements x_i of the matrix $\boldsymbol{X}_b$ represent whether the battery i has been removed from the circuit, with $x_i = 1$ indicating removal and $x_i = 0$ indicating that it is still available to supply power. When all batteries are health and capable of providing current to the external load, $\boldsymbol{X}_b$ is an identity matrix. The elements x_j of the matrix $\boldsymbol{X}_s$ represent whether the switch j is closed, with $x_j = 1$ indicating closure and $x_j = 0$ indicating disconnection, which is consistent with the previous subsection.

Theoretically, the output current I_o and the currents of each battery $\boldsymbol{I}_b$ in the RBS can be determined by solving Eqs. 4, 5, and 6 under any given state $\boldsymbol{X}$. In order to obtain specific constraint conditions and objective functions, it is further assumed that all batteries have the same electromotive force and internal resistance, denoted as u_b and r_b, respectively. This allows for the derivation of explicit expressions for I_o and $\boldsymbol{I}_b$. After derivation and simplification, the output current I_o and the currents of each battery $\boldsymbol{I}_b$ are ultimately represented as Eqs. 7 and 8, respectively.

$$I_o = \frac{1}{R_o r_b} \tilde{\boldsymbol{A}}_o^{\mathrm{T}} \boldsymbol{Y}_n^{-1}(\boldsymbol{X}) \tilde{\boldsymbol{A}}_b \boldsymbol{U}_b, \tag{7}$$

$$\boldsymbol{I}_b = \frac{1}{r_b^2} [\tilde{\boldsymbol{A}}_b^{\mathrm{T}} \boldsymbol{Y}_n^{-1}(\boldsymbol{X}) \tilde{\boldsymbol{A}}_b \boldsymbol{U}_b - r_b \boldsymbol{U}_b], \tag{8}$$

where $\boldsymbol{U}_b$ is a $N_b \times 1$ array with all elements equaling to u_b; $\boldsymbol{Y}_n$ is the equivalent admittance matrix of the circuit, defined as

$$\boldsymbol{Y}_n(\boldsymbol{X}) = \frac{1}{R_o} \tilde{\boldsymbol{A}}_o \tilde{\boldsymbol{A}}_o^{\mathrm{T}} + \frac{1}{r_b} \tilde{\boldsymbol{A}}_b \boldsymbol{X}_b \tilde{\boldsymbol{A}}_b^{\mathrm{T}} + \frac{1}{r_s} \tilde{\boldsymbol{A}}_s \boldsymbol{X}_s \tilde{\boldsymbol{A}}_s^{\mathrm{T}}. \tag{9}$$

To characterize the current output capacity of the RBS structure under different switching states, an indicator η is defined by the ratio of I_o and $\max(\boldsymbol{I}_b)$ shown in Eq. 10:

$$\eta = \frac{I_o}{\max(\boldsymbol{I}_b)}. \tag{10}$$

Finally the problem of solving MAC can be formulated as

$$\max \eta(\boldsymbol{X}_s) \tag{11}$$

$$\mathrm{s.t.} \max(\boldsymbol{I}_b) \leq I_m, \tag{12}$$

7

where I_m is the maximum allowable current of the battery.

However, it is computationally difficult to solve 11 because of the $\boldsymbol{Y}_n^{-1}$. On one hand, due to the introduction of nonlinear terms by $\boldsymbol{Y}_n^{-1}$, many effective methods in linear optimization are not suitable for this problem. On the other hand, the rank of Y_n is proportional to the number of batteries and switches, which can be very large for a large RBS system, leading to significant computational burden. Therefore, intelligent algorithms that rely on evolving by iteration may face efficiency issues when dealing with large RBS system. In order to address this issue, the problem should be considered from the perspective of guiding the RBS to reconstruct as many parallel structures as possible. Consequently, a greedy algorithm based on the shortest path is proposed. The detailed implementation process is presented in the following two subsections.

2.3   Shortest Path

The path p used in this method is defined as the complete route that passes through one battery (or a consecutive series of batteries) and closed switches, connecting the anode v_1 to the cathode v_N of the RBS. By applying a penalty to the series-connected batteries on the path, where additional batteries imply a longer distance, the algorithm encourages the RBS to form parallel structures as much as possible. Meanwhile, to reduce the number of switches controlled during the reconstruction process, a penalty is also applied to the total number of switches on the path, while ensuring the minimum number of batteries. Therefore, the distance ω of the path p is defined by the following equation:

$$\omega(p) = N_s \cdot n_b(p) + n_s(p), \tag{13}$$

where N_s is the total number of switches in the system; $n_b(p)$ and $n_s(p)$ are number of batteries and switches in the path p respectively. Moreover, the shortest path SP_i is defined as the path with the minimum ω for battery i, as shown in the following equation:

$$SP_i = \underset{p \in P_i}{\arg\min} \, \omega(p), \tag{14}$$

where P_i is the set of all paths from v_1 to v_N which pass through the directed edge i.

The SP_i can be solved by the Dijkstra algorithm. The Dijkstra algorithm is a graph search method that finds the shortest path between two given nodes in a weighted graph, efficiently solving the single-source shortest path problem. Assuming that the cathode and anode of battery i are denoted as v_i^- and v_i^+ respectively, the path p of battery i can be divided into three segments : $v_1 \to v_i^-$, $v_i^+ \to v_N$, and $v_i^- \to v_i^+$. The $v_i^- \to v_i^+$ is the directed edge corresponding to battery i. With the Dijkstra algorithm, shortest paths for the $v_1 \to v_i^-$ and $v_i^+ \to v_N$ can be calculated under the weights given in Eq. 13, denoted as $SP(v_i^- \to v_i^+)$ and $SP(v_i^+ \to v_N)$, respectively. Finally, the SP_i for battery i is formed by the complete path with $SP(v_1 \to v_i^-)$, $v_i^- \to v_i^+$, and $SP(v_i^+ \to v_N)$.

The Dijkstra algorithm can be used to implement the SP_i.

According to the definition, SP_i gives the simplest strategy by which the control of battery i is achieved with a minimum of switches while minimizing the influence of other batteries. From the perspective of series/parallel, the more batteries are connected into circuit via their SPs, the more batteries are connected in parallel.

2.4 Greedy Algorithm

In this subsection, a greedy algorithm is proposed based on shortest paths (SPs), which is given here firstly.

Since batteries can provide more total output current when connected in parallel than in series, the algorithm greedily selects as many cells as possible to be connected into to the overall circuit via their SPs to obtain the MAC.

The dichotomy method is also performed to faster find the right number of SPs. After finding the potential SPs combinations in correspondence MAC, the state variable $\boldsymbol{X}_s$ of the switches can be determined, and the optimization problem 11 can be solved using Eq. 10, 7 and 8. The overall flowchart is shown in Fig. 4, and the corresponding pseudo-code of the algorithm is shown in Appendix 1.

3 Case Study

In this section, an intricate structure shown in Fig. 4 is constructed based on the combination of two RBS structures, which are plotted in Fig. (a) and (b) respectively. … The new proposed RBS structure integrates the advantages of these two traditional RBS structures, and is particularly used to demonstrate the use of the proposed MAC determination method.

3.1 Determination of a new RBS structure

The RBS structure proposed by Lawson et al[8], shown in Fig. 1b, easily enables the isolation of the highly degraded battery (or a series connection of batteries) from the battery module. In contrast, the structure proposed by Visairo et al[9], shown in Fig. 1a, allows the flexibility to switch the cells between series, parallel and mixed series-parallel modes, thus allowing dynamic voltage adjustment according to the external load and improving energy conversion efficiency, but is not as simple as the structure by Lawson et al in terms of isolating cells or adding redundancy. In order to combine the advantages of both above RBS structures, a new structure is obtained by integrating the Visairo RBS structure into Lawson RBS structure as shown in Fig. 5a. In this way, the circuit topology of the substructure (for instance the batteries B1, B2 and their related switches) can be changed to enable dynamic and flexible voltage tuning in terms of the external load, as well as taking advantage of the ease of battery isolation and increased redundancy of the main frame.
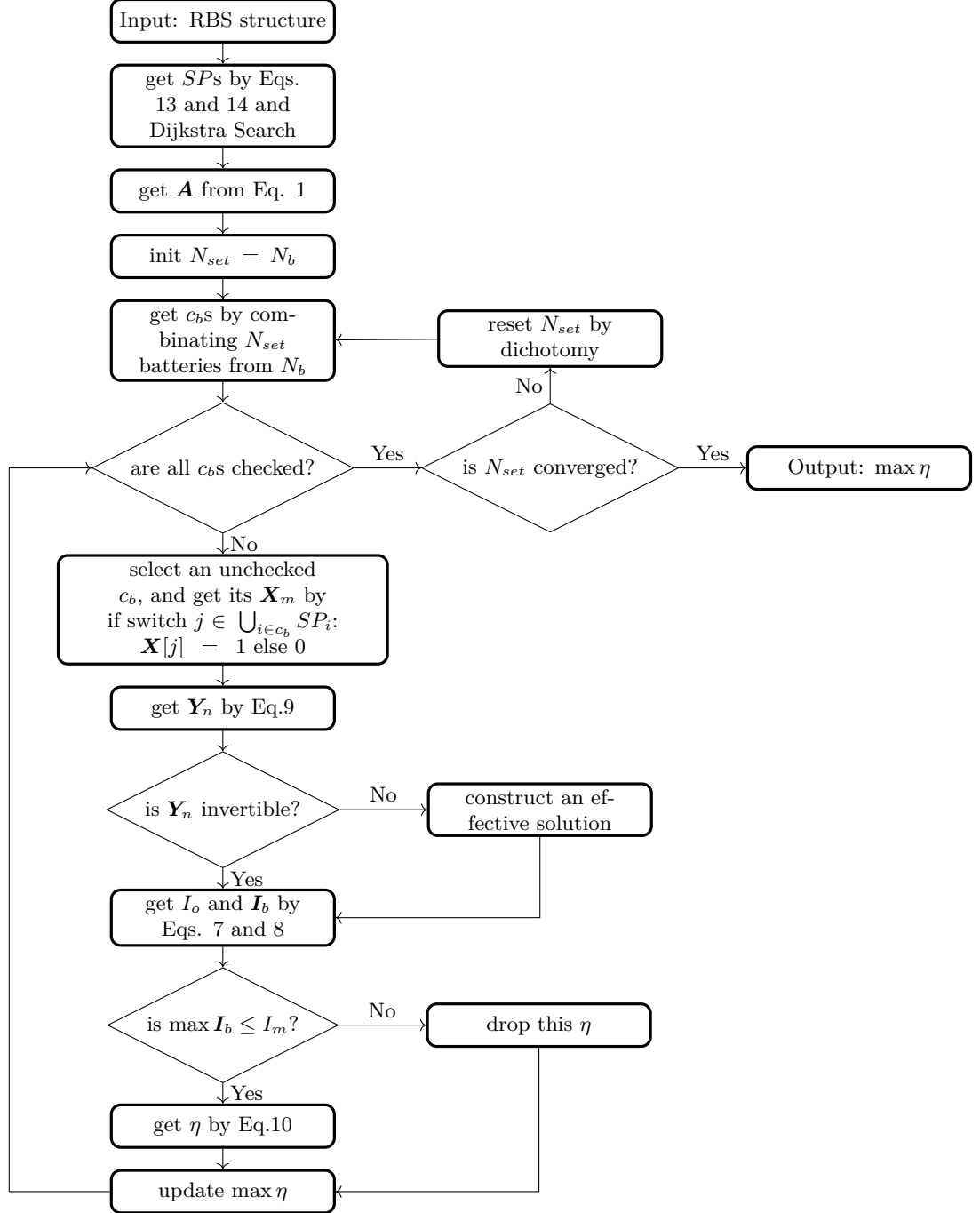
Input: RBS structure

get SPs by Eqs. 13 and 14 and Dijkstra Search

get $\boldsymbol{A}$ from Eq. 1

init $N_{set} = N_b$

get c_bs by combinating N_{set} batteries from N_b

reset N_{set} by dichotomy

are all c_bs checked? — Yes → is N_{set} converged? — Yes → Output: $\max \eta$

No (from is N_{set} converged? up to reset N_{set} by dichotomy)

No → select an unchecked c_b, and get its $\boldsymbol{X}_m$ by if switch $j \in \bigcup_{i \in c_b} SP_i$: $\boldsymbol{X}[j] = 1$ else 0

get $\boldsymbol{Y}_n$ by Eq.9

is $\boldsymbol{Y}_n$ invertible? — No → construct an effective solution

Yes → get I_o and $\boldsymbol{I}_b$ by Eqs. 7 and 8

is $\max \boldsymbol{I}_b \leq I_m$? — No → drop this η

Yes → get η by Eq.10

update $\max \eta$

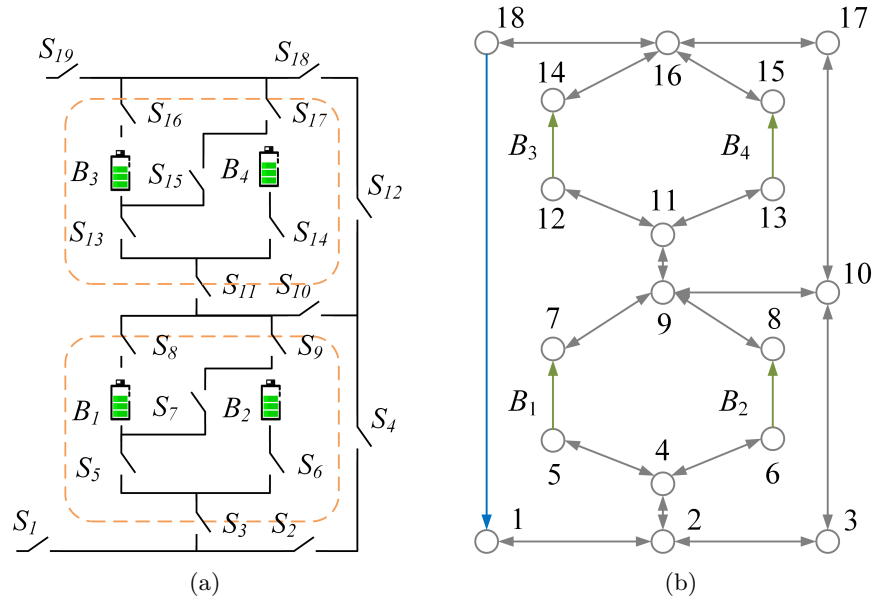Figure 4: The computational flowchart of the MAC if an RBS.

10

Figure 5: (a) The new RBS structure proposed by ... (b) The corresponding topologic model of the new RBS structure, which is a directed graph. The nodes represent the connection points of the battery cells and/or the switches. The green,gray and blue directed edges represent the battery cells, the switches and the external electrical load, respectively.

3.2 Result

The directed graph in Fig. 5b represents the topology of the new RBS structure proposed in this study (Fig. 5a). In this model, batteries B_1, B_2, B_3, and B_4 are represented by green directed edges in the graph, while 19 switches are represented by gray directed edges with two-way directions. The external electrical load is considered as a directed edge from the cathode of the RBS (i.e. node 18) to the anode (i.e. node 1), represented as the blue directed edge in the graph.

Based on the node-edge relationship given in Fig. 5b, the incidence matrix $\boldsymbol{A}$ can be obtained according to Eq. 1:

$$\boldsymbol{A} = \begin{bmatrix} \boldsymbol{A}_b & \boldsymbol{A}_s & \boldsymbol{A}_o \end{bmatrix}, \tag{15}$$

$$\boldsymbol{A}_b^{\mathrm{T}} = \begin{bmatrix} 0 & 0 & 0 & 0 & 1 & 0 & -1 & 0 & 0 & 0 & 0 & 0 & 0 & 0 & 0 & 0 & 0 \\ 0 & 0 & 0 & 0 & 0 & 1 & 0 & -1 & 0 & 0 & 0 & 0 & 0 & 0 & 0 & 0 & 0 \\ 0 & 0 & 0 & 0 & 0 & 0 & 0 & 0 & 0 & 0 & 0 & 1 & 0 & -1 & 0 & 0 & 0 \\ 0 & 0 & 0 & 0 & 0 & 0 & 0 & 0 & 0 & 0 & 0 & 0 & 1 & 0 & -1 & 0 & 0 \end{bmatrix}, \tag{16}$$

$$\boldsymbol{A}_s^{\mathrm{T}} = \begin{bmatrix} 1 & -1 & 0 & 0 & 0 & 0 & 0 & 0 & 0 & 0 & 0 & 0 & 0 & 0 & 0 & 0 & 0 \\ 0 & 1 & -1 & 0 & 0 & 0 & 0 & 0 & 0 & 0 & 0 & 0 & 0 & 0 & 0 & 0 & 0 \\ 0 & 1 & 0 & -1 & 0 & 0 & 0 & 0 & 0 & 0 & 0 & 0 & 0 & 0 & 0 & 0 & 0 \\ 0 & 0 & 1 & 0 & 0 & 0 & 0 & 0 & 0 & -1 & 0 & 0 & 0 & 0 & 0 & 0 & 0 \\ 0 & 0 & 0 & 1 & -1 & 0 & 0 & 0 & 0 & 0 & 0 & 0 & 0 & 0 & 0 & 0 & 0 \\ 0 & 0 & 0 & 1 & 0 & -1 & 0 & 0 & 0 & 0 & 0 & 0 & 0 & 0 & 0 & 0 & 0 \\ 0 & 0 & 0 & 0 & 1 & 0 & 0 & -1 & 0 & 0 & 0 & 0 & 0 & 0 & 0 & 0 & 0 \\ 0 & 0 & 0 & 0 & 0 & 0 & 1 & 0 & -1 & 0 & 0 & 0 & 0 & 0 & 0 & 0 & 0 \\ 0 & 0 & 0 & 0 & 0 & 0 & 0 & 1 & -1 & 0 & 0 & 0 & 0 & 0 & 0 & 0 & 0 \\ 0 & 0 & 0 & 0 & 0 & 0 & 0 & 0 & 1 & -1 & 0 & 0 & 0 & 0 & 0 & 0 & 0 \\ 0 & 0 & 0 & 0 & 0 & 0 & 0 & 0 & 1 & 0 & -1 & 0 & 0 & 0 & 0 & 0 & 0 \\ 0 & 0 & 0 & 0 & 0 & 0 & 0 & 0 & 0 & 1 & 0 & 0 & 0 & 0 & 0 & 0 & -1 \\ 0 & 0 & 0 & 0 & 0 & 0 & 0 & 0 & 0 & 0 & 1 & -1 & 0 & 0 & 0 & 0 & 0 \\ 0 & 0 & 0 & 0 & 0 & 0 & 0 & 0 & 0 & 0 & 1 & 0 & -1 & 0 & 0 & 0 & 0 \\ 0 & 0 & 0 & 0 & 0 & 0 & 0 & 0 & 0 & 0 & 0 & 1 & 0 & 0 & -1 & 0 & 0 \\ 0 & 0 & 0 & 0 & 0 & 0 & 0 & 0 & 0 & 0 & 0 & 0 & 0 & 1 & 0 & -1 & 0 \\ 0 & 0 & 0 & 0 & 0 & 0 & 0 & 0 & 0 & 0 & 0 & 0 & 0 & 0 & 1 & -1 & 0 \\ 0 & 0 & 0 & 0 & 0 & 0 & 0 & 0 & 0 & 0 & 0 & 0 & 0 & 0 & 0 & 1 & -1 \\ 0 & 0 & 0 & 0 & 0 & 0 & 0 & 0 & 0 & 0 & 0 & 0 & 0 & 0 & 0 & 1 & 0 \end{bmatrix}, \tag{17}$$

$$\boldsymbol{A}_o^{\mathrm{T}} = \begin{bmatrix} -1 & 0 & 0 & 0 & 0 & 0 & 0 & 0 & 0 & 0 & 0 & 0 & 0 & 0 & 0 & 0 & 0 & 0 \end{bmatrix}. \tag{18}$$

The state matrix $\boldsymbol{X}$ is determined by the switches' state, that is, the specific configuration of the RBS. For example, when switch S_1, S_3, S_5, S_6, S_8, S_9, S_{11},

S_{13}, S_{14}, S_{16}, S_{17} and S_{19} are ON, and the rest of the switches are OFF, the state matrix $\boldsymbol{X}$ is given by

$$\boldsymbol{X} = diag(\underbrace{1,0,1,0,1,1,0,1,1,0,1,0,1,1,0,1,1,0,1}_{\text{switches}}, \underbrace{1,1,1,1}_{\text{batteries}}, 1). \qquad (19)$$

By substituting the above specific values of $\boldsymbol{A}$ and $\boldsymbol{X}$ above into Eqs. 9, 7, 8 and 10 in turn, the η at the current situation, i.e. battery cell B_1 and B_2, B_3 and B_4 are connected in parallel with each other, and then connected in series to supply the external electrical appliance, can be obtained after the sequential calculation. The results are shown in Tab. 1.

Table 1: Calculating result of the output current I_o, battery current $\boldsymbol{I}_b$ and ratio η for a specificed switches state $\boldsymbol{X}_m$ in the structure combining Lawson et al.[8] and Visairo et al.[9] with 4 battery cells and 19 switches.

Structure	4 battery cells and 19 switches
Switch ON	1,3,5,6,8,9,11,13,14,16,17,19
$\boldsymbol{X}_s$	diag$(1,0,1,0,1,1,0,1,1,0,1,0,1,1,0,1,1,0,1)$
I_o	$2u_b/(R_o + r_b)$
$\boldsymbol{I}_b$	$[u_b/(R_o + r_b), u_b/(R_o + r_b), u_b/(R_o + r_b), u_b/(R_o + r_b)]$
η	2

The above gives the procedure for calculating the current and η when the specified switches are given ON or OFF. However, in order to calculate the MAC of the structure, i.e. the maximum η, it is necessary to find the corresponding switch state using a greedy strategy, as mentioned in subsection 2.4.

Firstly, the weight N_s in Eq. 13 represents the total number of switches in the system, which is 19. By using this formula and the Dijkstra search strategy, the SPs of each cell can be obtained, as shown in Figs. 6a to 6d. According to the greedy strategy, as many SPs as possible should be selected to get the MAC. In the first iteration, the SPs of all four batteries are selected, and the switch states on the paths are set to ON. The corresponding $\boldsymbol{X}_s$ are calculated using the previous method, and the currents of the batteries are obtained as u_b/r_b, u_b/r_b, u_b/r_b, and u_b/r_b. Since all batteries are short-circuited and the current of the battery exceeds the maximum allowed current I_m, this solution does not satisfy constraint 12 and is discarded. The second iteration is carried out using the dichotomy method, and two batteries are selected for the combination. Assuming that the selected combinations are $(B1, B2)$, the $\boldsymbol{X}_s$ obtained according to the SPs are substituted into the previous calculation, and the current of each battery is u_b/r_b, u_b/r_b, 0, and 0. This solution meets the condition. After that, the case of selecting three cells is considered. By similar calculations, it is determined that all solutions do not satisfy the constraint when three cells are selected. Finally, the MAC of this structure is $\eta = 2$, and the related result is shown in Fig. 7 and Tab. 2.
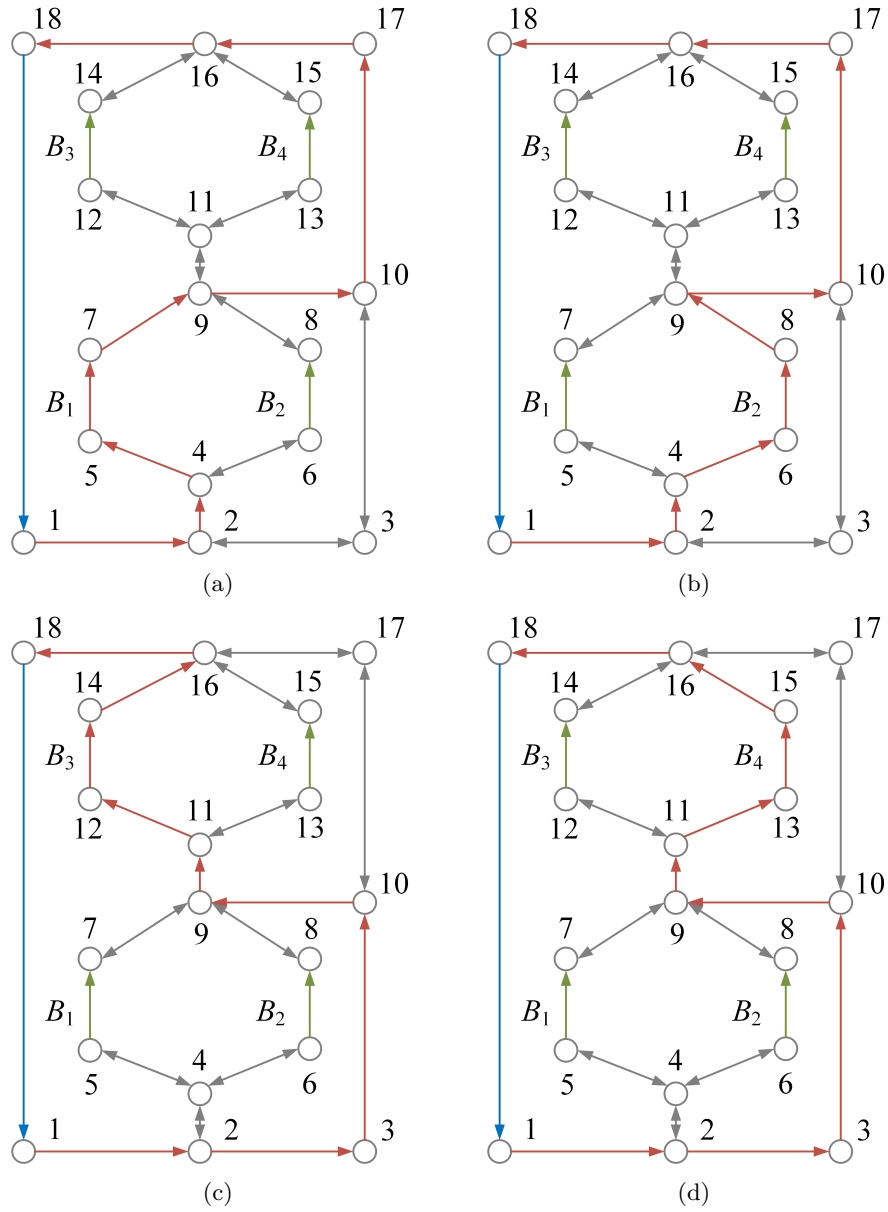
Figure 6: The SPs (highlighted in red) of battery (a)B_1 (b)B_2 (c)B_3 (d)B_4 in the complex RBS structure

14

Table 2: MAC Calculating result of the output current I_o, battery current $\boldsymbol{I}_b$ and ratio η in the structure combining Lawson et al.[8] and Visairo et al.[9] with 4 battery cells and 19 switches.

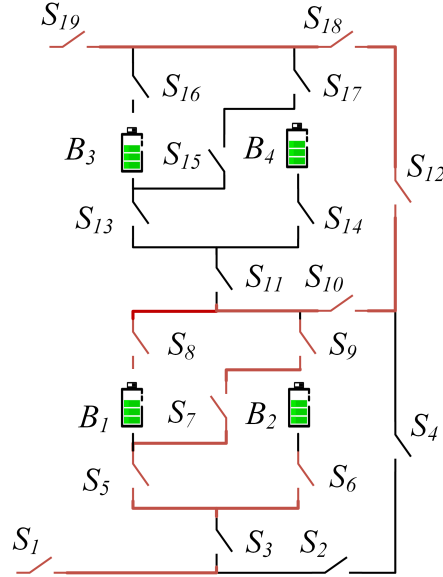| Structure	4 battery cells and 19 switches
Switch ON	1,3,5,6,8,9,10,12,18,19
$\boldsymbol{X}_s$	$\mathrm{diag}(1,0,1,0,1,1,0,1,1,1,0,1,0,0,0,0,0,1,1)$
I_o	$2u_b/(2R_o+r_b)$
$\boldsymbol{I}_b$	$[u_b/(2R_o+r_b),u_b/(2R_o+r_b),0,0]$
η	2

Figure 7: The finally calculation result of MAC for the new structure with four battery cells and 19 switches. The red lines represent the branches through which the current flows, and the switches on these branches are ON. In this situation, the RBS outputs MAC to the outside, which is $\eta = 2$.

3.3   Discussion

First, the correctness of the results in Fig. reffig:ef-mac is discussed here. When B_1 and B_2 or B_3 and B_4 are connected in parallel, the RBS can output the maximum current, which is $\eta = 2$, i.e. twice the current output of a single battery in RBS. While adding more batteries to the main circuit can only form a series structure and will not improve the MAC. It is worth noting that when solving for MAC, η is used as the objective function instead of I_o, which makes the result of MAC more reasonable. According to the results shown in Tab. 2, I_o and $\boldsymbol{I}_b$ are affected by the equivalent resistance R_o of external electrical appliance, the battery's electromotive force u_b, and internal resistance r_b. This means that if I_o is used as the objective function, even for the same RBS structure, the MAC result and corresponding switch state could be changed due to different external electrical appliances. This increases the difficulty and uncertainty in RBS structure design. On the contrary, by using η as the objective function, which dividing I_o and max $\boldsymbol{I}_b$, the influence of these factors on the results is eliminated, as shown in Tabs. 1 and 2. η only reflects the maximum output current capability of the RBS structure. Assuming that the maximum allowed current of battery cells in the RBS is I_m, the maximum output current of the RBS structure can be calculated as ηI_m by calculating the η of the structure. Therefore, compared to I_o, η is more suitable for structure design. Most of the currently proposed RBS structures[12, 13, 14, 15, 16, 17] have simple topological characteristics, and the calculation of MACs are relatively simple, even intuitive. However, when complex and flexible structures need to be designed for application scenarios such as equalization or isolation of specific battery cells, the estimation of MAC will become complex and complicated. The method proposed in this paper can effectively solve any RBS structure and estimate MAC universally, paving the way for the structure design of more complex and flexible RBSs.

When the RBS has isolated battery cells, the original topology of the structure is altered. However, the method proposed in this paper can still be used to calculate the MAC of the new structure. The MAC after the isolation operation can be obtained by calculating the new structure following the procedures described in the previous subsection. During the calculation process, the isolated battery cell(s) do not participate in the calculation, i.e., their nodes, edges, and SPs are not considered. The MACs under various isolated battery cell(s) are calculated on the structures proposed by Lawson et al. (Fig. 1b), Visairo et al. (Fig. 1a), and the new structure that integrates the previous two structures (Fig. 5b), as shown in Fig. 8. For the structure proposed by Lawson et al., the MAC remains the same as that without isolated battery cells, i.e., $\eta = 1$, when the number of isolated battery cells increases, until all the cells in the RBS are isolated. For the structure proposed by Visairo et al., the MAC decreases as the number of isolated battery cells increases, until $\eta = 0$. While the new structure has two cases of isolating two cells, one is to isolate two cells within the same substructure, in which case $\eta = 2$; the other is to isolate one cell in each of the two substructures, in which case $\eta = 1$. Overall, the MAC of the new structure is positioned between the structures proposed by Lawson et al. and Visairo et

16

al.. It can be seen that the MAC of the structure in Fig. 1b is the most stable, and the structure has advantages in isolation and redundancy backup, but its MAC is the smallest. The structure proposed shown by Fig. 1a can output the largest MAC but is susceptible to the number of isolated battery cells. However, the structure proposed by this paper has certain advantages in both aspects, being insensitive to the number of isolated battery cells while simultaneously achieving a larger MAC.
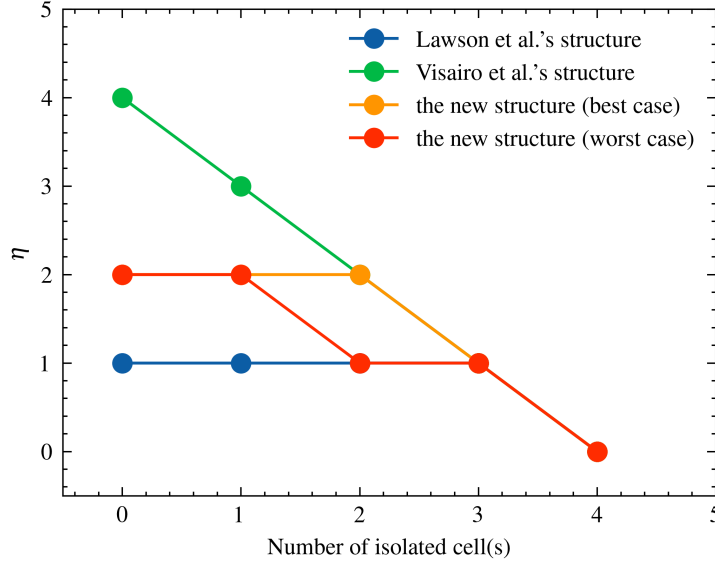

Figure 8: The variation of MAC with the number of isolated battery cells for different RBS structures, including the structure proposed by Lawson et al., Visairo et al. , and the new structure in this paper.

4 Conclusion

This paper firstly proposes a method to calculation the MAC of RBS according to its architecture. To find the circuit in RBS that enable the MAC, a greedy strategy incorporate with the topologic model is developed to. The effectiveness of proposed method is tested on a more complex RBS structure based on two proposed structure. This work presents an effective approach to evaluate the MAC of RBS, which is essential for design and management of the RBS. Future research could focus on developing new performance indicators for evaluating RBS performance using the currents and voltages obtained by this method, as well as modifying the equivalent model of the battery to enable more accurate simulations of RBS, including transient analysis.

5 Appendix

Algorithm 1: Get the max available currents of a certain RBS

Data: Directed graph model $G(V, E)$ of the RBS
Result: $\max \eta$

1 **for** $i \in E_b$ **do**
2     $P_i \leftarrow \{path | \text{starts at } v_1 \text{ and ends at } v_n\}$;
3     $SP_i \leftarrow p_i$ which has the minimum $\omega(p_i)$ among all $p_i \in P_i$.
4 **end**
5 get $\boldsymbol{A}$ by Equation 1;
6 **while** *not yet determine* $\max \eta$ **do**
7     $N_{sel} \leftarrow$ number of selected SPs calculated by dichotomy;
8     $C_b \leftarrow$ set of all combinations of N_{sel} batteries from N_b;
9   **for** $c_b \in C_b$ **do**
10        $\boldsymbol{x}_s \leftarrow$ list of all switches' state: $x_s[j] = 1$ if $j \in \bigcup_{i \in c_b} SP_i$ else 0;
11        $\boldsymbol{X} \leftarrow diag[1, 1, \cdots, 1, \boldsymbol{x}_s]$;
12   get $\boldsymbol{Y}_n$ by Equation 9;
13   **if** $\boldsymbol{Y}_n$ *is invertible* **then**
14   **else**
15   construct an effective solution
16   **end**
17   get I_o by Equation 7;
18   get $\boldsymbol{I}_b$ by Equation 8;
19   **if** $\max(\boldsymbol{I}_b) \leq I_m$ **then**
20           $\eta \leftarrow I_o / \max(\boldsymbol{I}_b)$;
21   **else**
22   break
23   **end**
24   **end**
25 **end**

6 Acknowledgement

References

[1] p. u. family=Siqueira, given=Luanna Maria Silva and W. Peng, "Control strategy to smooth wind power output using battery energy storage system: A review," vol. 35, p. 102252.

[2] R. Karandeh, T. Lawanson, and V. Cecchi, "A Two-Stage Algorithm for Optimal Scheduling of Battery Energy Storage Systems for Peak-Shaving," in *2019 North American Power Symposium (NAPS)*, pp. 1–6.

[3] Y. Yang, S. Bremner, C. Menictas, and M. Kay, "Battery energy storage system size determination in renewable energy systems: A review," vol. 91, pp. 109–125.

[4] J. Cho, S. Jeong, and Y. Kim, "Commercial and research battery technologies for electrical energy storage applications," vol. 48, pp. 84–101.

[5] N. Yang, X. Zhang, B. Shang, and G. Li, "Unbalanced discharging and aging due to temperature differences among the cells in a lithium-ion battery pack with parallel combination," vol. 306, pp. 733–741.

[6] F. Feng, X. Hu, L. Hu, F. Hu, Y. Li, and L. Zhang, "Propagation mechanisms and diagnosis of parameter inconsistency within Li-Ion battery packs," vol. 112, pp. 102–113.

[7] W. Han, T. Wik, A. Kersten, G. Dong, and C. Zou, "Next-Generation Battery Management Systems: Dynamic Reconfiguration," vol. 14, no. 4, pp. 20–31.

[8] B. Lawson, "A Software Configurable Battery,"

[9] H. Visairo and P. Kumar, "A reconfigurable battery pack for improving power conversion efficiency in portable devices," in *2008 7th International Caribbean Conference on Devices, Circuits and Systems*, pp. 1–6, IEEE.

[10] H. He, R. Xiong, X. Zhang, F. Sun, and J. Fan, "State-of-Charge Estimation of the Lithium-Ion Battery Using an Adaptive Extended Kalman Filter Based on an Improved Thevenin Model," vol. 60, no. 4, pp. 1461–1469.

[11] S. Mousavi G. and M. Nikdel, "Various battery models for various simulation studies and applications," vol. 32, pp. 477–485.

[12] S. Ci, J. Zhang, H. Sharif, and M. Alahmad, "A Novel Design of Adaptive Reconfigurable Multicell Battery for Power-Aware Embedded Networked Sensing Systems," in *IEEE GLOBECOM 2007-2007 IEEE Global Telecommunications Conference*, pp. 1043–1047.

[13] M. Alahmad, H. Hess, M. Mojarradi, W. West, and J. Whitacre, "Battery switch array system with application for JPL's rechargeable micro-scale batteries," vol. 177, no. 2, pp. 566–578.

[14] H. Kim and K. G. Shin, "Dependable, efficient, scalable architecture for management of large-scale batteries," in *Proceedings of the 1st ACM/IEEE International Conference on Cyber-Physical Systems*, ICCPS '10, pp. 178–187, Association for Computing Machinery.

[15] Y. Kim, S. Park, Y. Wang, Q. Xie, N. Chang, M. Poncino, and M. Pedram, "Balanced reconfiguration of storage banks in a hybrid electrical energy storage system," in *2011 IEEE/ACM International Conference on Computer-Aided Design (ICCAD)*, pp. 624–631.

[16] T. Kim, W. Qiao, and L. Qu, "A series-connected self-reconfigurable multicell battery capable of safe and effective charging/discharging and balancing operations," in *2012 Twenty-Seventh Annual IEEE Applied Power Electronics Conference and Exposition (APEC)*, pp. 2259–2264.

[17] L. He, L. Kong, S. Lin, S. Ying, Y. Gu, T. He, and C. Liu, "Reconfiguration-assisted charging in large-scale Lithium-ion battery systems," in *2014 ACM/IEEE International Conference on Cyber-Physical Systems (ICCPS)*, pp. 60–71.